

1

2 **Attention-dependent preparatory processing of naturalistic narratives is**
3 **correlated with speech comprehension**

4

5 Jiawei Li^{1,3}, Bo Hong^{2,3}, Guido Nolte⁴, Andreas K. Engel⁴, Dan Zhang^{1,3*}

6 ¹Department of Psychology, School of Social Sciences, Tsinghua University, Beijing,
7 China

8 ²Department of Biomedical Engineering, School of Medicine, Tsinghua University,
9 Beijing, China

10 ³Tsinghua Laboratory of Brain and Intelligence, Tsinghua University, Beijing, China

11 ⁴Department of Neurophysiology and Pathophysiology, University Medical Center
12 Hamburg Eppendorf, Hamburg, Germany

13

14 *Correspondence:

15 Dan Zhang, Ph.D.

16 Room 334, Mingzhai Building, Tsinghua University, Beijing 100084, China

17 E-mail: dzhang@tsinghua.edu.cn; Tel: +86-10-62796737

18 **Abstract**

19 While human speech comprehension is thought to be an active process that involves
20 top-down predictions, it remains unclear how predictive information is used to prepare
21 for the processing of upcoming speech information. We aimed to identify the neural
22 signatures of preparatory processing of upcoming speech. Participants selectively
23 attended to one of two competing naturalistic, narrative speech streams, and a temporal
24 response function method was applied to derive event-related-like neural responses
25 from electroencephalographic data. Regression analysis revealed that neural signatures
26 with latencies as early as -450 ms prior to speech onset were significantly correlated
27 with speech comprehension performance. The preparatory process involved a
28 distributed network. These preparatory signatures were attention dependent; activity
29 prior to the attended speech was negatively correlated with comprehension performance,
30 whereas the opposite was found for unattended speech. Our findings suggest that
31 attention plays an important role in the preparation to process upcoming speech.

32

33 **Keywords**

34 preparatory processing, attention, speech comprehension, electroencephalogram,
35 temporal response function

36

37

38 **Introduction**

39 Humans are a powerful speech recognition system that can comprehend complex and
40 rapidly changing human speech in challenging conditions, e.g., in a cocktail party
41 scenario with multiple competing speech streams and high background noise. To
42 achieve such a capacity, the human brain is equipped with neural architecture that is
43 dedicated to bottom-up processing of perceived speech information, from the low-level
44 acoustics, to the phoneme, syllable, and sentence levels (DeWitt & Rauschecker, 2012;
45 Friederici, 2012; Hickok, 2012a; Pisoni & Luce, 1987; Verhulst, Altoè, & Vasilkov,
46 2018). In recent years, increasing evidence has also suggested that human speech
47 comprehension is an active process that involves top-down predictions (Arnal, Wyart,
48 & Giraud, 2011; Federmeier, 2007; Fries, 2015; Hickok, Houde, & Rong, 2011; Kutas
49 & Federmeier, 2011; Rao & Ballard, 1999; Tian, Ding, Teng, Bai, & Poeppel, 2018). In
50 the cocktail party scenario, it is believed that a listener should continuously predict what
51 their attended speaker is going to say next to efficiently understand the corresponding
52 speech (Cherry, 1953; O’Sullivan et al., 2015; Zion Golumbic, Cogan, Schroeder, &
53 Poeppel, 2013). These predictions supposedly inform the brain about the ‘what’ and
54 ‘when’ of upcoming speech information (Arnal & Giraud, 2012; Auksztulewicz et al.,
55 2018), which allows a listener to prepare for follow-up processing.

56 Although the idea of top-down prediction in human speech comprehension is gaining
57 popularity, it remains unclear how the brain uses predictive information to prepare for
58 the processing of upcoming speech information. Understanding the preparatory process
59 is essential because it reflects the influence of prediction on subsequent information

60 processing. Moreover, the available findings on prediction in speech are not sufficient
61 to determine the neural mechanisms underlying preparation. For instance, the classic
62 studies of active speech prediction have mainly focused on the neural activity in
63 response to prediction errors. Event-related potential (ERP) components such as the
64 N400 and P600 are frequently reported when the perceived word violates semantic and
65 syntactic congruency of the preceding speech context, respectively (Kutas &
66 Federmeier, 2011; Lau, Phillips, & Poeppel, 2008; Van Petten & Luka, 2012). These
67 ERP components normally occur >400 ms after the presentation of the perceived speech,
68 and so provide only indirect support for the preparatory process. Recent studies have
69 also reported evidence of the brain's pre-activation before the onset of the upcoming
70 speech (DeLong, Urbach, & Kutas, 2005; Dikker & Pylkkänen, 2013; Söderström,
71 Horne, Frid, & Roll, 2016; Söderström, Horne, Mannfolk, van Westen, & Roll, 2018);
72 these pre-activations have been interpreted as 'predictive' because they have been found
73 to be correlated with the relative likelihoods of the upcoming speech unit (e.g. words)
74 in the continuous speech materials (e.g. sentences). However, this is still only indirect
75 evidence for preparation, as these pre-activations have been represented by event-
76 related neural responses to the preceding speech unit that are informative about possible
77 upcoming speech units. Direct neural evidence for the preparatory response should be
78 derived from neural activity that is directly related to the processing of the upcoming
79 speech information, and which occurs immediately before speech onset.

80 While this direct evidence has not been investigated in the speech domain, several
81 studies on general sensory processing have provided ample support for the existence of

82 such a preparatory process. For instance, pre-stimulus oscillatory activity has been
83 reported to have a significant impact on subsequent perceptual consequences (Cao,
84 Thut, & Gross, 2017; Galindo-Leon et al., 2019; Harris, Dux, & Mattingley, 2018; Kok,
85 Mostert, & De Lange, 2017; Rassi, Wutz, Müller-Voggel, & Weisz, 2019). Moreover,
86 synchronization within neural populations responsible for the specific sensory
87 processing has been proposed to underlie preparation (Engel, Fries, & Singer, 2001;
88 Galindo-Leon et al., 2019; Lakatos et al., 2009). Following on from this work, the
89 present study investigated neural activity prior to the onset of upcoming speech
90 information to identify possible neural signatures of the preparatory process.

91 One crucial issue that needs to be considered is the possible dependence of the
92 preparatory process on top-down selective attention. As attention regulates the
93 processing of the input sensory information, it can be expected to affect prediction and
94 consequently preparation. Indeed, recent studies have demonstrated the interplay
95 between attention and prediction (Schröger, Kotz, & SanMiguel, 2015; Schröger,
96 Marzecová, & Sanmiguel, 2015). Specifically, the magnitude of the prediction error-
97 related neural response has been shown to be magnified or reversed, depending on the
98 attentional state (Auksztulewicz & Friston, 2015; Hisagi, Shafer, Strange, & Sussman,
99 2015; Kok, Jehee, & de Lange, 2012; Marzecová, Widmann, SanMiguel, Kotz, &
100 Schröger, 2017; Smout, Tang, Garrido, & Mattingley, 2019). Most of these studies have
101 been conducted within the visual domain, with limited exploration in the auditory
102 domain, let alone speech processing. Compared to vision, the fast temporal dynamics
103 of auditory stimuli and speech signals require neuroimaging tools such as EEG that can

104 track online changes in neural activity with a high temporal resolution.

105 The present study aimed to identify neural signatures that directly reflect the
106 preparatory processing of human speech. A 60-channel electroencephalogram (EEG)
107 was recorded from participants while they listened to naturalistic narratives; this
108 procedure is believed to be of high ecological validity and thus to provide necessary
109 contextual information for the engagement of top-down prediction and therefore
110 preparation (Federmeier, 2007; Friston, 2005; Jehee & Ballard, 2009; Rao & Ballard,
111 1999). A cocktail party paradigm was used, whereby we introduced a complex
112 perceptual environment that imposed further demands on prediction and preparation
113 (Broderick, Anderson, Di Liberto, Crosse, & Lalor, 2018). To obtain the neural
114 responses to continuous, naturalistic speech, we used a temporal response function
115 (TRF) method, to derive event-related-like neural responses from EEG data, for both
116 the attended and unattended speech streams in the cocktail party scenario (Crosse, Di
117 Liberto, Bednar, & Lalor, 2016; Lalor, Pearlmuter, Reilly, McDarby, & Foxe, 2006).

118 Following studies on the perceptual influence of pre-stimulus neural activities (Iemi et
119 al., 2019; Rassi et al., 2019; Smith, Johnstone, & Barry, 2006), these TRF-based
120 responses were analyzed for neural signatures related to speech comprehension
121 performance, as measured by speech-content-related questionnaires. We considered
122 that performance-relevant TRF-based responses before speech onset would be direct
123 neural evidence for the preparatory process, as the comparison between the predicted
124 and the actual perceived sensorial information cannot be performed during this period.

125 Furthermore, our experimental design allows the investigation on the attention

126 dependence of preparatory speech processing. Specifically, regression analyses were
127 employed with the TRF-based neural responses to attended and unattended speech
128 streams as the independent variables, and speech comprehension performance as the
129 dependent variable. Results revealed that neural signatures with latencies as early as -
130 450 ms prior to speech onset were significantly correlated with speech comprehension
131 performance. A distributed network was involved in the preparatory process of speech
132 comprehension. The preparatory activity to the attended speech was found to be
133 negatively correlated with comprehension performance, whereas the opposite was
134 found for unattended speech. Our findings suggest that attention plays an important role
135 in the preparation to process upcoming speech.

136 **Results**

137 Twenty participants took part in 28 'cocktail party' trials. In each trial, two narrative
138 stories were presented simultaneously to both the left and the right ears and the
139 participants were instructed to attend to one spatial side. Comprehension performance
140 was evaluated by questionnaires about the story contents, which were implemented at
141 the end of each story. There were two four-choice questions for the two simultaneously
142 heard stories, respectively. The comprehension performance was significantly better for
143 the 28 attended stories than for the 28 unattended stories ($67.0 \pm 2.5\%$ (standard error)
144 vs. $36.0 \pm 1.6\%$; the four-choice chance level: 25%; $t(19) = 10.95$, $p < .001$). The
145 participants reported a moderate level of attention (8.15 ± 0.34 on a 10-point Likert scale)
146 and attention difficulties (2.04 ± 0.53 on a 10-point Likert scale). The accuracy for the
147 attended story was significantly correlated with both the self-reported attention level (r

148 = .476, $p = .043$) and attention difficulty ($r = -.677, p = .001$). The self-reported story
149 familiarity level was low for all the participants (0.86 ± 0.22 on a 10-point Likert scale)
150 and was not correlated with comprehension performance ($r = -.224, p = .342$). These
151 results suggest that participants' selective attention was effectively manipulated, as well
152 as good reliability of the measured comprehension performance. Most importantly,
153 there was a large inter-individual difference in the participant-wise average
154 comprehension performance for the attended stories; the response accuracy varied from
155 48.2% to 91.1%, which supports the feasibility of using these accuracy values as a
156 behavioral indicator of comprehension-relevant neural signatures.

157 The analysis workflow is shown in Figure 1. TRF-derived neural responses to the
158 attended and unattended speech were calculated separately, at latencies of -500 ms to
159 500 ms relative to speech onset. Responses within the -500–0 ms latency window are
160 considered to represent preparatory activity, whereas responses within the 0–500 ms
161 latency window reflect post-processing of the speech stream. These TRF responses also
162 underwent time-frequency analysis, and the average single-trial amplitudes and inter-
163 trial phase-locking (ITPL) values were calculated. We hypothesized that this
164 decomposition into amplitude and phase responses would yield more detailed insights
165 into the underlying neural mechanisms of speech processing, as amplitude and phase
166 have been proposed to play unique roles in networks underlying human cognition
167 (Engel, Gerloff, Hilgetag, & Nolte, 2013; Fries, 2015; Klimesch, 2012). To achieve this,
168 we established linear regression models with either amplitude or phase responses from
169 both the attended and unattended TRFs as the independent variables, and

170 comprehension accuracy of the attended speech as the dependent variable. The TRF-
171 based amplitude and phase responses at different channels, latencies, and frequencies
172 were used in separate regression models. We used regression analysis to take a full
173 consideration of possible joint contributions from the attended and unattended TRFs,
174 by deriving different regression coefficients respectively. The regression analyses were
175 performed by treating each participant's comprehension accuracy averaged over all the
176 28 attended stories as the dependent variable. This provides a robust estimation of the
177 comprehension performance, as only two four-choice questions were asked per
178 attended story. In addition, this design could allow more flexibility in neural data
179 analysis, e.g. exploring the inter-story variability in phase responses.

180 Regression models were built separately for the neural responses at each channel-
181 latency-frequency bin. The regression *R*-values were obtained to reveal how well the
182 regression models correlated with individual comprehension performance. Statistical
183 analyses were performed based on these regression *R*-values using a nonparametric
184 cluster-based permutation method (Maris & Oostenveld, 2007). Any significant results
185 at a latency <0 ms were taken to indicate the neural correlates of preparation for
186 upcoming speech information. We also calculated the mean of the regression coefficient,
187 and drew the distribution for every cluster.

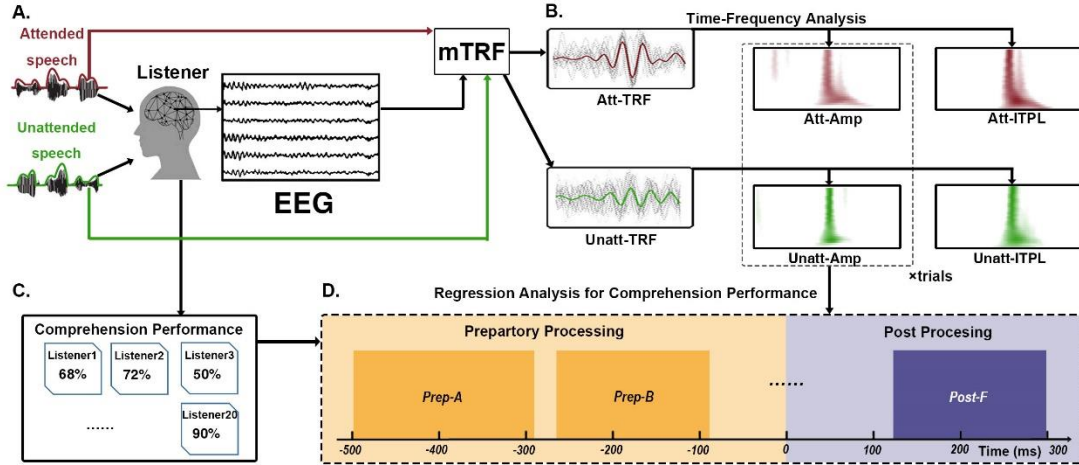


Figure 1. The analysis workflow

(A) The experimental paradigm. Participants attended to one of two simultaneously presented naturalistic, narrative speech streams while 60-channel EEG was recorded. (B) EEG data analysis. Neural responses were characterized using a TRF-based modeling method. The TRF-based neural responses were then further subjected to a time-frequency analysis at the single-trial level and decomposed into single-trial amplitude and phase (by inter-trial phase locking, ITPL) responses based on the time-frequency representations (denoted by ‘Amp’ and ‘ITPL’). This procedure was conducted for attended (Att-) and unattended (Unatt-) speech streams separately. (C) Comprehension performance. The participants completed a comprehension task after each speech comprehension trial. The average response accuracy over all trials per participant was taken as comprehension performance. (D) Regression analysis for comprehension performance-related neural responses. We established linear regression models with either amplitude or phase responses from both the attended and unattended TRFs as the independent variables, and comprehension accuracy of the attended speech as the dependent variable, for each channel-latency-frequency bin. The neural responses with significant regression model fitting are reported. We defined neural activity before 0 ms as preparatory processing and activity after 0 ms as post processing.

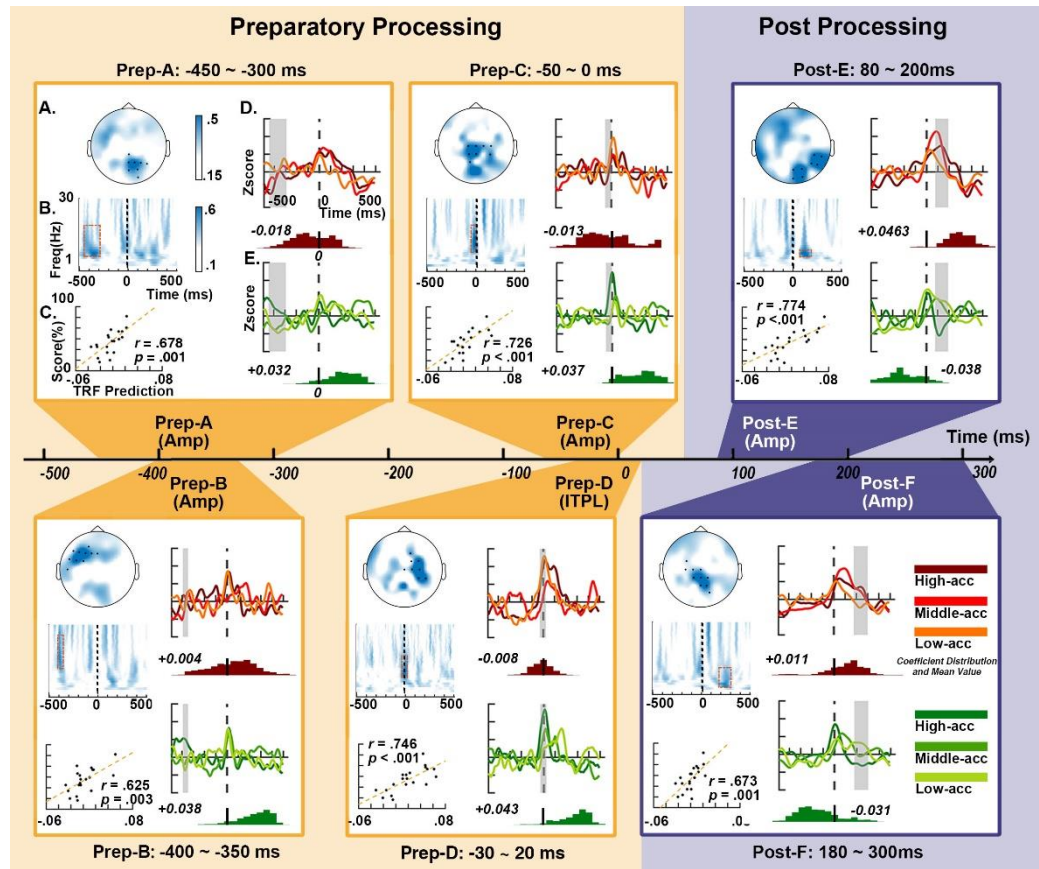
Preparatory neural activities were correlated with speech comprehension performance

The nonparametric cluster-based permutation analysis revealed a significant correlation between the multi-channel time-frequency representation of the TRFs and individual speech comprehension performance of the attended speech. This corresponded to six

213 clusters in the observed data (all, $p < .05$), as shown in Figure 2.

214 There were four clusters with latencies prior to 0 ms, which suggested that the brain
215 actively prepares for upcoming speech information. The earliest cluster (*Prep-A*)
216 extended from around -450 ms to -300 ms, and spread from the theta to low beta range
217 (6–18 Hz) over the right parietal region (permutation $p = .005$). The average prediction
218 model within the cluster revealed a significant correlation between the predicted and
219 the actual comprehension performance ($r = .678, p = .001$). The following cluster (*Prep-*
220 *B*) extended from around -400 ms to -350 ms, and spread from the alpha to beta range
221 (12–25 Hz) over the left frontal region (permutation $p = .030$; model prediction $r = .625,$
222 $p = .003$). There were two clusters with latencies around 0 ms. While *Prep-C* was based
223 on amplitude responses, much like *Prep-A* and *Prep-B*, *Prep-D* was based on the ITPL.
224 The amplitude cluster (*Prep-C*) extended from -50 ms to 0 ms, and spread from the
225 alpha to low beta range (9–19 Hz) over the central-parietal region (permutation $p = .015$;
226 model prediction $r = .725, p < .001$). The ITPL cluster (*Prep-D*) extended from -30 ms
227 to 20 ms, and spread from the alpha to low beta range (10–17 Hz) over the right central
228 region (permutation $p = .002$; model prediction $r = .746, p < .001$).
229 There were also two clusters with latencies >0 ms. The first cluster (*Post-E*) occurred
230 at 80–200 ms, and spread within the alpha range (7–9 Hz) over the right temporal region
231 (permutation $p = .035$; model prediction $r = .774, p < .001$). The other cluster (*Post-F*)
232 occurred at 180–300 ms, and spread from the theta to alpha range (4–11 Hz) over the
233 central parietal region (permutation $p = .008$; model prediction $r = .673, p = .001$).
234 These clusters were speech-following responses that likely reflect post processing of

235 the speech information for comprehension.



236

237 **Figure 2. Neural responses that were correlated with speech comprehension**
238 **performance**

239 There are six clusters showing significant correlations with the comprehension
240 performance of the attended speech, shown as six sub-plots. Each sub-plot is divided
241 into five panels (A~E, labeled only in the upper left sub-plot titled 'Prep-A'), as
242 explained below.

243 (A) Grand average topography of the regression R -values in the time windows of the
244 significant clusters (depicted by the gray shadowed area in (D) and (E)). Black dots
245 indicate the channels of interest included in these clusters.

246 (B) Time-frequency profile of the R -values averaged over the channels of interest. The
247 dashed red rectangles indicate the time and frequency of interest included in the clusters.

248 (C) Scatter plots of the comprehension performance (y-axis) and the predicted values
249 by the regression model averaged over all the channel-latency-frequency bins within
250 the corresponding clusters (x-axis). Each dot represents an individual participant.

251 (D) and (E) Response time courses of attended-TRF(D) and unattended-TRF(E). The
252 three red (D) and green (E) lines of different darkness represent the averaged responses
253 over the participants with comprehension performance of the attended speech ranking
254 in the top, middle, and bottom tertiles (7, 6, and 7 participants, respectively). The

255 histograms illustrate the distribution of coefficients of the selected channel-latency-
256 frequency bins. The number displayed beside the histogram is the mean regression
257 coefficient within the selected channel-latency-frequency bins.

258 **Preparatory activities were attention dependent**

259 The regression models for both attended and unattended responses revealed a joint
260 contribution of the preparatory activities related to the attended and the unattended
261 speech streams for the speech comprehension performance. For all six clusters, the
262 mean regression coefficients within the selected channel-latency-frequency bins were
263 significantly different from zero. For example, the mean of the coefficients for the
264 attended and unattended activities of *Prep-A* were -0.018 and 0.032, respectively (the
265 99% bootstrap confidence intervals for the attended activity: [-0.019, -0.016]; for
266 unattended activity: [+0.030, +0.033]; for all means and distributions, see Fig. 2D and
267 2E). Thus, both the attended and unattended activities significantly contributed to
268 individual comprehension performance. By plotting the average TRF responses within
269 the channel-latency-frequency of interest in these clusters for the participants with
270 comprehension performance ranking in the top, middle, and bottom tertiles, we
271 observed primarily reversed trends for the attended and unattended responses.
272 Interestingly, reduced preparatory activities to the attended speech were seen for the
273 top-performance tertile (corresponding to the negative mean coefficients), whereas the
274 opposite effect was seen for the unattended speech (except for *Prep-B*, in which both
275 mean coefficients were positive). The post-processing activities showed the reverse
276 pattern, whereby participants with a better performance exhibited enhanced responses
277 to the attended speech (as reflected by positive mean coefficients) and reduced

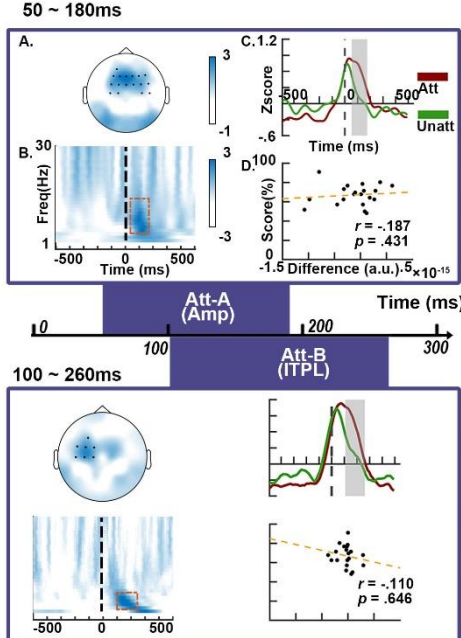
278 responses to the unattended speech (as reflected by negative mean coefficients). The
279 99% bootstrap confidence intervals for the means of all the coefficients are provided in
280 Table S1.

281 We further computed partial correlations between these preparatory neural activities
282 and the comprehension performance, while controlling for the post-processing neural
283 activities (i.e., *Post-E* and *Post-F*). *Prep-B* and *Prep-C* had significant partial
284 correlations with the comprehension performance ($r = .610$ and $.560$, $p = .007$ and $.016$,
285 respectively), which is suggestive of a unique functional contribution to comprehension
286 performance of the two preparatory neural responses. The partial correlations of *Prep-*
287 *A* and *Prep-D* with the comprehension performance failed to reach significance ($r = .32$
288 and $.44$, $p = .189$ and $.068$, respectively). Nevertheless, as these preparatory activities
289 occurred substantially earlier than the post-processing activities, the non-significant
290 results do not necessarily undermine the importance of these responses, but rather
291 indicate there to be shared neural mechanisms for preparation and post-processing.
292 Indeed, both the spectral and spatial signatures of *Prep-A* and *Post-F* largely overlapped,
293 and *Prep-D* and *Post-E* shared similar spatial patterns. In support of these observations,
294 significant correlations were found between *Prep-A* and *Post-F* ($r = .648$, $p = .002$) and
295 between *Prep-D* and *Post-E* ($r = .672$, $p = .001$). The pairwise correlations between all
296 six clusters are shown in Table S2, and the partial correlation results are shown in Table
297 S3.

299 **Attention modulation was reflected by post-onset processing: replication of**
300 **previous TRF-based studies**

301 Several previous studies have employed a similar paradigm to investigate the
302 attentional modulation of speech processing (Broderick et al., 2018; Mirkovic, Debener,
303 Jaeger, & Vos, 2015; O’Sullivan et al., 2015). In these studies, the attentional
304 modulation effect was operationalized as the difference between TRF responses to
305 attended and unattended speech, whereas the present study focused on neural signatures
306 that were associated with speech comprehension performance. To replicate their
307 findings, we computed the attention-related neural activities according to these
308 previous studies.

309 To this end, a cluster-based permutation analysis was performed to search for
310 differences between the TRF-based neural responses to the attended and unattended
311 speech, based on the multichannel time-frequency responses of either amplitude or
312 phase responses. Selective attention resulted in significant differences the neural
313 activities related to the attended and unattended speech streams, as represented by an
314 amplitude-based cluster and a phase-based cluster. Both clusters had latencies well after
315 0 ms. Compared to the unattended speech, the attended speech was associated with a
316 larger amplitude response at 50–180 ms at 5–13 Hz over the parietal region ($p = .018$)
317 and a stronger ITPL at 100–260 ms at 4–8 Hz over the left-central parietal region (p
318 $= .028$). None of the clusters, however, were significantly correlated with speech
319 comprehension performance ($r = -.110$ and $-.187$, $p = .646$ and $.431$).



320

321 **Figure 3. Attention-related neural responses were not correlated with speech**
322 **comprehension performance**

323 There are two clusters showing significant difference between attended and unattended
324 speech streams. Each sub-plot is divided into four panels (A~D, labeled only in the
325 upper sub-plot), as explained below.

326 (A) Grand average topography of *t*-values on the difference between the attended and
327 unattended responses in the time windows of the significant clusters (depicted by the
328 gray shadowed area in (C)). Black dots represent the channels of interest.

329 (B) Time-frequency profile of the *t*-values averaged over the channels of interest. The
330 dashed red rectangles indicate the time and frequency of interest included in the clusters.

331 (C) Grand average time courses of the attended (red) and unattended (green) TRF
332 responses averaged over the channels and frequencies of interest. Gray shaded areas
333 indicate the time windows of interest.

334 (D) Scatter plots of the comprehension performance (y-axis) and the response
335 differences averaged over all channel-latency-frequency bins within the corresponding
336 clusters (x-axis). Each dot represents one participant.

337

338 **Discussion**

339 The present study aimed to identify neural signatures that directly reflect preparatory
340 processing of upcoming speech. We used naturalistic narrative speech materials in a

341 selective attention paradigm using a TRF-based approach for modeling the neural
342 activity, and observed preparatory neural activities before the onset of speech power
343 envelope fluctuations. These preparatory activities were correlated with the
344 comprehension performance of individual participants, with latencies as early as -450
345 ms. The preparatory process involved spatially distributed brain areas, taking the form
346 of an amplitude response rather than phase synchronization, with the most relevant
347 frequencies within the alpha and beta ranges. There was also an interplay between
348 attention and preparation, whereby preparatory activities to the attended and the
349 unattended speech contributed to comprehension performance, but with opposite
350 mechanisms. Our results provide direct neural evidence for how the brain prepares for
351 the processing of upcoming speech.

352 Before detailed discussions, it is necessary to state that our assumption for a preparatory
353 process is based on the observation that the TRF-based neural activities prior to speech
354 onset were significantly correlated with comprehension performance. Recent TRF-
355 based studies using naturalistic stimuli have reported reasonable latencies that
356 resembled their ERP counterparts for describing selective auditory attention (~200 ms)
357 (Mirkovic et al., 2015; O'Sullivan et al., 2015), semantic violation processing (~400
358 ms) (Broderick et al., 2018), and visual working memory (200–400 ms) (Huang, Jia,
359 Han, & Luo, 2018). Although our findings have mainly focused the window of < 0 ms,
360 these studies support the rationale of using the TRF-based responses to reflect the time
361 course of information processing in general. Therefore, the pre-onset latencies observed
362 in the present study can be considered to represent a preparatory state that precedes

363 speech processing.

364 **Preparatory activities involve a distributed neural network**

365 To prepare for the processing of upcoming speech information, multiple neural
366 signatures with different time, space, and frequency characteristics were identified,
367 which is indicative of the engagement of multi-center neural networks for active speech
368 perception. We did not base our analysis on preselected regions of interest, and so our
369 results provide a complete overview of all activities for preparation. Notably, one
370 preparatory cluster was found to be located over the left frontal region (*Prep-B*), which
371 supports the popular notion of a left-lateralized frontal network for top-down speech
372 prediction (Federmeier, 2007; Hickok, 2012b). Previous studies that have reported
373 involvement of the left frontal region in prediction have focused on post-processing of
374 either violations of linguistic congruency (e.g. the MMN and N400 responses; (Kutas
375 & Hillyard, 1984; Lau et al., 2008; Szewczyk & Schriefers, 2018) or contextual speech
376 cues (Dikker & Pylkkänen, 2013; Söderström et al., 2016). However, our results
377 indicate that this region plays an active role in preparation of speech processing, with
378 latencies of ~400 ms before speech onset.

379 Furthermore, the preparatory process was broadly distributed beyond the left frontal
380 region, including the parietal (*Prep-A*), central-parietal (*Prep-C*), and right central
381 (*Prep-D*) regions. The central-parietal responses could be related to the predictive
382 processing of speech meaning, and could recruit a mechanism that is similar to that
383 underlying the classical central-parietal N400 response (Federmeier, 2007; Lau et al.,

384 2008; Szewczyk & Schriefers, 2018). The right-lateralized finding (i.e., *Prep-D*),
385 however, may indicate a possible functional contribution of the right hemisphere to
386 prediction. Some studies have suggested that the right hemisphere is engaged in
387 language processing, primarily during complex narratives (Brownell HH, Michel D,
388 Powelson J, & Gardner H, 1983; George, Kutas, Martinez, & Sereno, 1999; Robertson
389 et al., 2000). As naturalistic speech materials used in the present study were likely to
390 engage speech processing at all levels, our results demonstrate the involvement of a
391 distributed neural network for the preparation of naturalistic speech processing.

392 **Higher frequency neural activity for preparation and lower frequency activity for
393 post-processing**

394 The neural mechanisms of the preparatory process were investigated using a time-
395 frequency analysis of the TRF-based neural activity. Similarly to recent TRF-based
396 studies, we observed attention-related neural responses (Mirkovic, Bleichner, De Vos,
397 & Debener, 2016; Mirkovic et al., 2015; O'Sullivan et al., 2015), with the peak attention
398 effect represented by theta and alpha oscillatory activities at 100–200 ms post-stimulus
399 onset over the frontal regions. Similarly, the comprehension-related post-onset
400 processing was mainly reflected in lower frequency bands from theta to low alpha
401 bands, as has been frequently reported in previous speech literatures (Ding & Simon,
402 2014; Giraud & Poeppel, 2012; Luo & Poeppel, 2007). In contrast, the comprehension-
403 related pre-onset neural signatures were in a higher frequency range, mainly within the
404 alpha and beta bands. This observation is in accordance with recent studies on pre-
405 stimulus ERPs in sensory perception, in which pre-stimulus alpha-band activity was

406 found to be significantly correlated with post-stimulus perception, especially in the
407 visual modalities (Bauer, Stenner, Friston, & Dolan, 2014; Milton & Pleydell-Pearce,
408 2016; Rohenkohl & Nobre, 2011; van Ede, Jensen, & Maris, 2010). These results have
409 been interpreted for a functional role of alpha band for a top-down inhibitory
410 mechanism to achieve the preparatory process. Meanwhile, several studies have
411 suggested that beta-band power reflects updating the content of a prediction (Bauer et
412 al., 2014; Sedley et al., 2016), as well as maintenance of ongoing cognitive context
413 (Engel & Fries, 2010). Accordingly, the pre-onset alpha and beta activity in our study
414 may reflect inhibitory of unattended speech and maintain the expectation in speech
415 preparatory processing (Kayser, Ince, Gross, & Kayser, 2015; Keitel, Gross, & Kayser,
416 2018). Taken together, these results suggest possibly of distinct functional roles of
417 neural activity at different frequency bands for speech processing, with alpha- or
418 higher-band activity reflecting top-down speech preparation, and the lower-frequency
419 activity reflecting post-stimulus processing.

420 In addition, three out of the four preparatory activities took the form of an amplitude
421 response rather than ITPL, including the earliest activities (*Prep-A* and *Prep-B*). At a
422 first glance, our observation may seem to be inconsistent with the popular view on the
423 functional roles of amplitude and phase responses, as phase synchronization is
424 frequently suggested to reflect the coordination of long-distance neuron communication
425 and therefore more likely to reflect top-down regulation of sensory information
426 processing (Engel et al., 2001, 2013; Galindo-Leon et al., 2019; Klimesch, 2012;
427 Lakatos et al., 2009; Salinas & Sejnowski, 2001; Sauseng et al., 2007; Schyns, Thut, &

428 Gross, 2011; Zhang, Hong, Gao, & Röder, 2017). Nevertheless, as the preparation
429 process reflects the usage of top-down predictive information for facilitated speech
430 processing rather than prediction *per se*, it is likely that these preparatory activities
431 mainly exhibited the actual implementation of prediction in speech-processing-specific
432 brain regions. In support of such a hypothesis, the distributed neural network indeed
433 covered the typical speech processing regions. Therefore, the amplitude-based
434 preparatory activities could be the result of localized speech-related information
435 processing as proposed in previous studies on general sensory processing (Engel et al.,
436 2001; Klimesch, Sauseng, & Hanslmayr, 2007; Mathewson et al., 2011; Zhang et al.,
437 2017). These activities could be related to the processing of the contextual information
438 relevant for the upcoming speech and thus provide the basis for the enhanced
439 comprehension performance. As limited previous studies have addressed the
440 dissociation between amplitude and phase responses, further work is necessary to
441 elucidate this issue.

442 **Attention dependence of the preparatory neural signatures**

443 The neural mechanisms of the preparatory process were further explored by inspecting
444 their relationship with attention. We further decomposed neural activity into amplitude
445 and phase responses. Specifically, our findings of the earliest preparation-related
446 amplitude modulation (*Prep-A*) in the alpha and beta bands support the recent reports
447 of beta power reduction during temporal prediction (Arnal & Giraud, 2012; Nobre &
448 Van Ede, 2018); in high-performing participants, comprehension performance was
449 associated with reduced amplitudes in response to attended speech and enhanced

450 amplitudes in response to unattended speech (i.e., the positive and negative regression
451 coefficients as displayed in Fig. 2D and 2E). Similar patterns were also seen for *Prep-*
452 *C* and *Prep-D* (ITPL in this case). The reduced amplitude responses and ITPL could
453 reflect a well-prepared state for processing upcoming attended speech (Bauer et al.,
454 2014; Chao, Takaura, Wang, Fujii, & Dehaene, 2018; Jensen & Mazaheri, 2010). The
455 neural activities related to the unattended speech were also correlated with speech
456 performance, but with opposite effects. Thus, the different modulation effects could
457 contribute towards an enlarged activity difference between the neural activities to the
458 attended and the unattended speech, for an efficient processing and thus comprehension
459 of the attended speech information.

460 Interestingly, although the neural activities related to both the attended and the
461 unattended speech also jointly contributed to comprehension performance at the post-
462 processing stage (*Post-E* and *Post-F*), a reversed pattern was observed as compared to
463 the preparatory stage. In participants with better performances, performance was
464 associated with enhanced responses to the attended speech and reduced responses to
465 the unattended speech. This reversed pattern is in accordance with the classical view
466 on attention modulation, and reflects enhanced processing to attended information and
467 suppressed processing to unattended information (Carrasco, 2011; Luck, Woodman, &
468 Vogel, 2000). The sharp contrast between the preparatory and the post-processing
469 processing stages supports the idea that there is an interplay between preparation and
470 attention. While our results are in line with previous research that has reported there to
471 be an interaction between attention and prediction (Friston, 2009; Kok, Rahnev, Jehee,

472 Lau, & de Lange, 2012; Smout et al., 2019), we provide further evidence on how such
473 interactions could affect behavior (i.e., comprehension). Namely, given that the
474 preparatory process supposedly reflects how prediction is implemented to facilitate
475 information processing, our results imply that attended speech may be favored by the
476 predictive or preparatory mechanism. Indeed, the neural activity associated with the
477 attended speech was inhibited during the preparatory stage, but enhanced during the
478 post processing stage, both mechanisms have been linked to more efficient processing
479 by previous studies (Rohenkohl & Nobre, 2011; Rommers, Dickson, Norton, Wlotko,
480 & Federmeier, 2017; Smith et al., 2006).

481 This study has some limitations that should be noted. The present study used the speech
482 power envelope as the reference signal from which the TRF models were derived,
483 which could reflect the speech information at all linguistic levels due to the highly
484 redundant information shared across levels (Daube, Ince, & Gross, 2019; Di Liberto,
485 O’Sullivan, & Lalor, 2015). While such an operation has the advantage of providing a
486 general overview about preparatory processing, further investigations are necessary to
487 differentiate possible contributions at different linguistic levels (Broderick et al., 2018;
488 Di Liberto et al., 2015). Meanwhile, caution must be taken when interpreting the timing
489 of the preparatory activities. While the preparatory activity as early as 450 ms before
490 speech onset could be the result of an optimized utilization of the rich contextual
491 information provided by the naturalistic speech materials, such timings may be
492 dependent upon the materials per se. Further studies are necessary to investigate the
493 possible material dependence of these timings, for instance, by employed an extended

494 amount of speech materials. In addition, an inter-individual level regression analysis
495 method was chosen, as the average comprehension questionnaire accuracies across all
496 stories within each participant was believed to provide a more reliable estimation the
497 speech comprehension performance than the single-trial accuracies. Thus, our results
498 do not necessarily imply that the observed neural signatures reflect the participants'
499 trait-like, stable speech processing style. Alternatively, it could be more plausible to
500 consider these neural signatures to reflect a more or less efficient speech processing
501 state. More theoretical and empirical research is needed to clarify the underlying
502 mechanisms.

503 **Summary**

504 We found that individual participants' comprehension performance was significantly
505 correlated with neural responses as early as -450 ms relative to speech onset. A widely
506 distributed brain network was involved in the preparatory process. Higher-frequency
507 activity in the alpha and beta bands were more closely related to top-down processing,
508 while lower-frequency activity was more closely associated with post processing.
509 Neural activities related to both the attended and the unattended speech contributed to
510 the comprehension performance, but with distinct mechanisms. Attended speech was
511 more efficiently processed when neural activity was inhibited in the preparatory stage
512 and enhanced during post processing, whereas the opposite effects were observed for
513 unattended speech. Our study provides a mechanistic description of how the brain
514 prepares to process upcoming speech information.

515 **Materials and Methods**

516 **Ethics statement**

517 The study was conducted in accordance with the Declaration of Helsinki and was
518 approved by the local Ethics Committee of Tsinghua University. Written informed
519 consent was obtained from all participants.

520 **Experimental model and participant details**

521 Twenty college students (10 female; mean age: 24.7 years; range: 20–43 years) from
522 Tsinghua University participated in the study as paid volunteers. All participants were
523 native Chinese speakers, reported having normal hearing, and had normal or corrected-
524 to-normal vision.

525 **Data acquisition and pre-processing**

526 EEG was recorded from 60 electrodes (FP1/2, FPZ, AF3/4, F7/8, F5/6, F3/4, F1/2, FZ,
527 FT7/8, FC5/6, FC3/4, FC1/2, FCZ, T7/8, C5/6, C3/4, C1/2, CZ, TP7/8, CP5/6, CP3/4,
528 CP1/2, CPZ, P7/8, P5/6, P3/4, P1/2, PZ, PO7/8, PO5/6, PO3/4, POZ, Oz, and O1/2),
529 which were referenced to a common average, with a forehead ground at Fz. A
530 NeuroScan amplifier (SynAmp II, NeuroScan, Compumedics, USA) was used to record
531 EEG at a sampling rate of 1000 Hz. Electrode impedances were kept below 10 kOhm
532 for all electrodes.

533 The recorded EEG data were first notch filtered to remove the 50 Hz powerline noise,
534 bandpass filtered to 0.5–40 Hz and then subjected to an artifact rejection procedure

535 using independent component analysis. Independent components (ICs) with large
536 weights over the frontal or temporal areas, together with a corresponding temporal
537 course showing eye movement or muscle movement activities, were removed. The
538 remaining ICs were then back-projected onto the scalp EEG channels, reconstructing
539 the artifact-free EEG signals. Around 4–9 ICs were rejected per participant.

540 Next, the EEG data were segmented into 28 trials according to the markers representing
541 speech onsets. The analysis window for each trial extended from 5 to 55 s (duration: 50
542 s) to avoid the onset and the offset of the stories.

543 **Stimuli**

544 The speech stimuli were recorded from two male speakers using the microphone of an
545 iPad2 mini (Apple Inc., Cupertino, CA) at a sampling rate of 44,100 Hz. The speakers
546 were college students from Tsinghua University, who had more than four years of
547 professional training in broadcasting. Both speakers were required to tell 28 1-min
548 narrative stories in Mandarin Chinese; the stories were either those about daily-life
549 topics recommended by the experimenter and told by the speaker improvising on their
550 own (14 stories), or those selected from the National Mandarin Proficiency Test (14
551 stories). The speakers were presented with the recommended topic or story materials
552 on the computer screen. They were allowed to prepare for as long as required before
553 telling the story (usually ~3 min). When they were ready, the speakers pressed the
554 SPACE key on the computer keyboard and the recording began with the presentation
555 of three consecutive pure-tone beep sounds at 1000 Hz (duration: 1000 ms; inter-beep

556 interval: 1500 ms). The beep sounds served as the event marker to synchronize the
557 speech audios in the main experiment, in which two speech streams were presented
558 simultaneously. The speakers were asked to start speaking as soon as the third beep had
559 ended (within around 3 sec). The speakers were allowed to start the recording again if
560 the audio did not meet the requirements of either the experimenter or the speakers
561 themselves (which mainly concerned speech coherence). The actual speaking time per
562 story ranged from 51 to 76 sec.

563 Two four-choice questions per story were then prepared by the experimenter and two
564 college students who were familiar with comprehension performance assessment.
565 These questions and the corresponding choices concerned story details that required
566 significant attentional efforts. For instance, one question following a story about one's
567 hometown was, "What is the most dissatisfying thing about the speaker's hometown?
568 (推测讲述人对于家乡最不满意的地方在于?)", and the four choices were A) There is no
569 heating in winter; B) There are no hot springs in summer; C) There is no fruit in autumn;
570 D) There are no flowers in spring (A. 冬天没暖气; B. 夏天没温泉; C. 秋天没水果; D.
571 春天没鲜花). Both the speech audio and corresponding questions are available for
572 downloads.

573 **Experimental procedure**

574 The main experiment consisted of 4 blocks of 7 trials. During each trial, two speech
575 streams were played simultaneously to the left and right ears. The two speech streams
576 within each trial were from the two different speakers to facilitate selective attention.

577 Considering the possible duration difference between the two audio streams, the trial
578 ended after the longer speech audio had ended. Each trial began when participants
579 pressed the SPACE key on the computer keyboard. Participants were instructed which
580 side to attend to by plain text (“Please pay attention to the [LEFT/RIGHT]”) displayed
581 on the computer screen. A white fixation cross was also displayed throughout the trial.
582 The speech stimuli were played immediately after the keypress, and were preceded by
583 the three beep sounds to allow participants to prepare. At the end of each trial, four
584 questions (two for each story) were presented sequentially in a random order on the
585 computer screen, and the participants made their choices using the computer keyboard.
586 After completing these questions, participants scored their attention level of the
587 attended stream, the experienced difficulty of performing the attention task, and the
588 familiarity with the attended material using three 10-point Likert scales. Throughout
589 the trial, participants were required to maintain visual fixation on the fixation cross
590 while listening to the speech and to minimize eye blinks and all other motor activity.
591 We recommended that participants take a short break (of around 1 min) after every trial
592 within one block, and a long break (no longer than 10 min) between blocks.
593 The to-be-attended side was fixed within each block (two blocks for attending to the
594 left side and two for attending to the right side). Within each block, the speaker identity
595 remained unchanged for the left and right sides. In this way, the to-be-attended spatial
596 side and the corresponding speaker identity were balanced within the participant, with
597 seven trials per side for both speakers. The assignment of the stories to the four blocks
598 was randomized across the participants.

599 The experiment was carried out in a sound-attenuated, dimly lit, and electrically
600 shielded room. The participants were seated in a comfortable chair in front of a 19.7-
601 inch Lenovo LT2013s Wide LCD monitor. The viewing distance was approximately 60
602 cm. The experimental procedure was programmed in MATLAB using the
603 Psychophysics Toolbox 3.0 extensions (Brainard & Brainard, 1997). The speech stimuli
604 were delivered binaurally via an air-tube earphone (Etymotic ER2, Etymotic Research,
605 Elk Grove Village, IL, USA) to avoid possible electromagnetic interferences from
606 auditory devices. The volume of the audio stimuli was adjusted to be at a comfortable
607 level that was well above the auditory threshold. Furthermore, the speech stimuli
608 driving the earphone were used as an analog input to the EEG amplifier through one of
609 its bipolar inputs together with the EEG recordings. In this way, the audio and the EEG
610 recordings were precisely synchronized, with a maximal delay of 1ms (at a sampling
611 rate of 1000 Hz).

612 **Temporal response function modeling**

613 The neural responses to the speech stimuli were characterized using a temporal
614 response function (TRF)-based modeling method. The TRF response describes the
615 impulse response to fluctuations of an input signal, and is based on system identification
616 theories (Crosse et al., 2016; Lalor et al., 2006). We used the power envelope of the
617 speech signal as the input signal required by TRF, which has been demonstrated to be
618 a valid index by which to extract speech-related neural responses (Bednar & Lalor,
619 2018; Broderick et al., 2018; Ding & Simon, 2012; Huang et al., 2018; Mirkovic et al.,
620 2015; O’Sullivan et al., 2015).

621 Prior to the modeling, the preprocessed EEG signals were re-referenced to the average
622 of all scalp channels and then downsampled to 128 Hz. Likewise, the power envelopes
623 of the speech signals were obtained using a Hilbert transform and then downsampled
624 to the same sampling rate of 128 Hz. When denoting the downsampled EEG signals
625 from channel i , trial k as $R(i,t)$ and the input speech power envelope as $S(t)$, the
626 corresponding neural response $TRF_{i,k}$ can be formulated as follows:

$$R(i,t) = TRF_{i,k} * S(t) \quad (1)$$

627 Where $*$ represents the convolution operator. The latency in the neural response models
628 ($TRF_{i,k}$) was set to vary from -1000 ms to 1000 ms post-stimulus to provide sufficient
629 data for the planned latency of -500 ms to 500 ms in the following time-frequency
630 analysis.

631 The TRF modeling analysis was performed on each EEG channel for each trial per
632 participant. TRF models were calculated for attended and unattended speech processing
633 separately using the corresponding speech streams as the input signal. It should be noted
634 that we did not consider the input lateralization for the TRF models, as the observed
635 behaviorally related findings were insensitive to the physical origin of the speech audios,
636 but rather likely to reflect the lateralization of the human speech network. Figure S3
637 provides the topographical information of our main results; it is similar to Figure 2, but
638 all results were calculated separately for speech stimuli from the left and right sides.
639 The topographies were comparable, even for the highly lateralized responses (e.g.,
640 *Prep-B and Post-E*).

641 The TRF-based neural responses were then further subjected to a time-frequency
642 analysis at the single-trial level. The TRF temporal profile was transformed using the
643 Hanning taper (2-cycle time window; for example, FWHM = 2 sec for 1 Hz wavelet)
644 at each time sample from -500 ms to 500 ms, with frequencies ranging from 1 to 30 Hz
645 at 1-Hz increments. Both single-trial amplitude and phase were recorded and denoted
646 as $TRF_{i,k}^A(\tau, f)$ and $TRF_{i,k}^P(\tau, f)$, where τ represents TRF latency relative to the onset
647 of speech power envelope fluctuations, and f represents the TRF frequency.
648 Given the number of trials denoted by N , the TRF-based single-trial amplitude and
649 phase responses were calculated as follows:

$$A_i(\tau, f) = \sum_{k=1}^N TRF_{i,k}^A(\tau, f) \quad (2)$$

$$ITPL_i(\tau, f) = \left| \sum_{k=1}^N \exp(j \cdot TRF_{i,k}^P(\tau, f)) \right| / N \quad (3)$$

650 A large-amplitude value indicates a neural response of high magnitude across all trials,
651 and the phase-related ITPL value varies between 0 and 1; 0 refers to a situation in which
652 the phase responses of different trials are uniformly distributed between 0 and 2π , and
653 1 means the phase responses from all trials are entirely locked to a fixed phase angle.
654 These phase and amplitude responses were further transformed into z-scores within the
655 -500 ms to 500 ms time window for each channel separately per participant. These z-
656 scores were then used for the cross-participant statistical analyses.
657 The TRF analysis was conducted in MATLAB using the Multivariate Temporal
658 Response Function (mTRF) toolbox (Crosse et al., 2016). All the other EEG processing

659 procedures, as well as the statistical analyses, were conducted using the FieldTrip
660 toolbox (Oostenveld, Fries, Maris, & Schoffelen, 2011).

661 **Quantification and statistical analysis**

662 The extracted TRF-based amplitude and phase responses were used as independent
663 variables into a regression model to predict the speech comprehension performance of
664 the attended speech at the participant level (denoted by *CompreScore*). Given that we
665 aimed to explore the neural correlates of speech comprehension, we built different
666 regression models for amplitude and phase responses, for each EEG channel (i) at
667 individual latency (τ) and frequency (f) separately. Nevertheless, the responses to the
668 attended and unattended speech streams were incorporated into the same regression
669 model, as follows:

$$CompreScore = \alpha_1 \cdot A_i^{Attended}(\tau, f) + \alpha_2 \cdot A_i^{Unattended}(\tau, f) \quad (4)$$

$$CompreScore = \alpha_1 \cdot ITPL_i^{Attended}(\tau, f) + \alpha_2 \cdot ITPL_i^{Unattended}(\tau, f) \quad (5)$$

670 Statistical analysis was performed to examine the significance of these regression
671 model predictions over all channel-latency-frequency bins by computing the regression
672 *R*-values. Nonparametric cluster-based permutation analysis was applied to control for
673 multiple comparisons. In this procedure, neighboring channel-latency-frequency bins
674 with an uncorrected *p*-value below 0.01 were combined into clusters, for which the sum
675 of correlational *t*-statistics corresponding to the regression *R*-values were obtained. A
676 null-distribution was created through permutations of data across participants ($n = 1000$

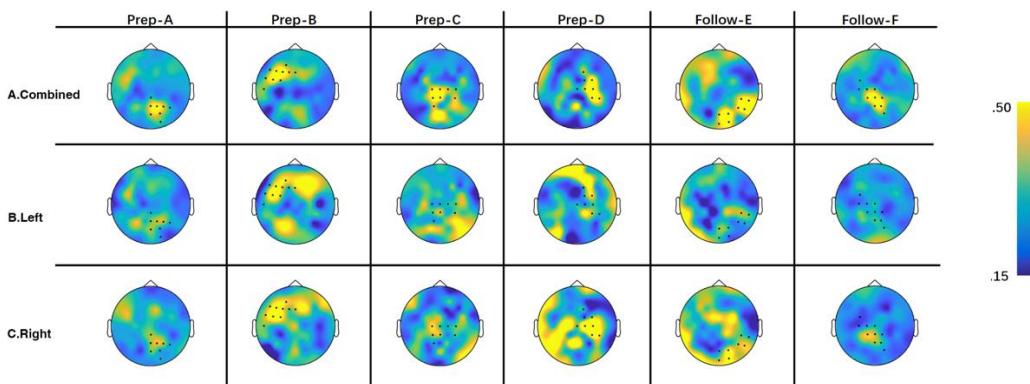
677 permutations), which defines the maximum cluster-level test statistics and corrected p -
678 values for each cluster.

679 We also examined the coefficients of the regression. We calculated the distribution and
680 the mean of every selected channel-latency-frequency bin. We also calculated 99%
681 regression coefficient confidence intervals using the bootstrap method for every cluster.

682 To investigate the attention modulation effect, we performed paired t-tests on the TRF-
683 based neural activities related to the attended speech versus the unattended speech. Both
684 amplitude and ITPL were included in the analysis. A similar cluster-based permutation
685 was used to control for the multiple comparison problem ($p < .01$ as the threshold, $n =$
686 1000 permutations).

687

688 **Supporting information**



690 Fig S1. Topographies of the six responses as shown in Figure 2 (A) and calculated
691 separately for the speech stimuli delivered to the left side (B) and the right side (C) only.

692

Table S1: Cls of all Clusters

	<i>Att</i>	<i>Unatt</i>
<i>Prep-A</i>	[-0.019, -0.016]	[+0.030, +0.033]
<i>Prep-B</i>	[+0.002, +0.007]	[+0.036, +0.040]
<i>Prep-C</i>	[-0.016, -0.009]	[+0.035, +0.040]
<i>Prep-D</i>	[-0.010, -0.006]	[+0.040, +0.045]
<i>Post-E</i>	[+0.044, +0.049]	[-0.041, -0.035]
<i>Post-F</i>	[+0.009, +0.013]	[-0.033, -0.029]

693

Table S2: Pairwise Correlation between all clusters

	<i>Prep-A</i>	<i>Prep-B</i>	<i>Prep-C</i>	<i>Prep-D</i>	<i>Post-E</i>
<i>Prep-B</i>	.589**				
<i>Prep-C</i>	.421	.439			
<i>Prep-D</i>	.480*	.408	.486*		
<i>Post-E</i>	.596**	.361	.474*	.672**	
<i>Post-F</i>	.648**	.378	.483*	.562**	.646**

** p<.01

* p<.05

694

Table S3: Partial correlation

	<i>Partial-r</i>	<i>p</i>
<i>Prep-A</i>	.323	.189
<i>Prep-B</i>	.560	.016*
<i>Prep-C</i>	.610	.007*
<i>Prep-D</i>	.439	.068

* p<.05

695

696

697 **Acknowledgments**

698 This work was supported by the National Science Foundation of China (NSFC) and the
699 German Research Foundation (DFG) in project Crossmodal Learning (grant number:
700 NSFC 61621136008/DFG TRR-169/C1, B1), the National Key Research and
701 Development Plan (grant number: 2016YFB1001200), the National Natural Science
702 Foundation of China (grant number: 61977041 and U1736220), and the National Social
703 Science Foundation of China (grant number: 17ZDA323).

704 The authors would like to thank Prof. Dr. Xiaoqin Wang and Dr. Yue Ding for providing
705 the shielded room for the experiment as well as necessary technical support.

706 **Author contributions**

707 J.L. conducted the experiments and data analysis; D.Z. designed the experiments and
708 wrote the paper; B.H., G.D., and A.K.E. edited the manuscript.

709 **Declaration of interests**

710 The authors declare no competing interests.

711

712 **References**

713 Arnal, L. H., & Giraud, A. L. (2012). Cortical oscillations and sensory predictions.
714 *Trends in Cognitive Sciences*, 16(7), 390–398.
715 <https://doi.org/10.1016/j.tics.2012.05.003>
716 Arnal, L. H., Wyart, V., & Giraud, A. L. (2011). Transitions in neural oscillations

717 reflect prediction errors generated in audiovisual speech. *Nature Neuroscience*,
718 14(6), 797–801. <https://doi.org/10.1038/nn.2810>

719 Auksztulewicz, R., & Friston, K. (2015). Attentional enhancement of auditory
720 mismatch responses: A DCM/MEG study. *Cerebral Cortex*, 25(11), 4273–4283.
721 <https://doi.org/10.1093/cercor/bhu323>

722 Auksztulewicz, R., Schwiedrzik, C. M., Thesen, T., Doyle, W., Devinsky, O., Nobre,
723 A. C., ... Melloni, L. (2018). Not all predictions are equal: “what” and “when”
724 predictions modulate activity in auditory cortex through different mechanisms.
725 *Journal of Neuroscience*, 38(40), 8680–8693.
726 <https://doi.org/10.1523/JNEUROSCI.0369-18.2018>

727 Bauer, M., Stenner, M. P., Friston, K. J., & Dolan, R. J. (2014). Attentional
728 modulation of alpha/beta and gamma oscillations reflect functionally distinct
729 processes. *Journal of Neuroscience*, 34(48), 16117–16125.
730 <https://doi.org/10.1523/JNEUROSCI.3474-13.2014>

731 Bednar, A., & Lalor, E. C. (2018). Neural tracking of auditory motion is reflected by
732 delta phase and alpha power of EEG. *NeuroImage*, 181, 683–691.
733 <https://doi.org/10.1016/j.neuroimage.2018.07.054>

734 Brainard, D. H., & Brainard, D. H. (1997). The Psychophysics Toolbox. In *Spatial
735 vision* (pp. 433–436).

736 Broderick, M. P., Anderson, A. J., Di Liberto, G. M., Crosse, M. J., & Lalor, E. C.
737 (2018). Electrophysiological Correlates of Semantic Dissimilarity Reflect the

738 Comprehension of Natural, Narrative Speech. *Current Biology*, 28(5), 803-

739 809.e3. <https://doi.org/10.1016/j.cub.2018.01.080>

740 Brownell HH, Michel D, Powelson J, & Gardner H. (1983). Surprise but not

741 coherence: sensitivity to verbal humor in right-hemisphere patients. *Brain and*

742 *Language*, 18(1), 20–27.

743 Cao, L., Thut, G., & Gross, J. (2017). The role of brain oscillations in predicting self-

744 generated sounds. *NeuroImage*, 147, 895–903.

745 <https://doi.org/10.1016/j.neuroimage.2016.11.001>

746 Carrasco, M. (2011). Visual attention: The past 25 years. *Vision Research*, 51(13),

747 1484–1525. <https://doi.org/10.1016/j.visres.2011.04.012>

748 Chao, Z. C., Takaura, K., Wang, L., Fujii, N., & Dehaene, S. (2018). Large-Scale

749 Cortical Networks for Hierarchical Prediction and Prediction Error in the

750 Primate Brain. *Neuron*, 100(5), 1252-1266.e3.

751 <https://doi.org/10.1016/j.neuron.2018.10.004>

752 Cherry, E. C. (1953). Some experiments on the recognition of speech, with one and

753 with two ears. *The Journal of the Acoustical Society of America*, 25, 975–979.

754 Crosse, M. J., Di Liberto, G. M., Bednar, A., & Lalor, E. C. (2016). The Multivariate

755 Temporal Response Function (mTRF) Toolbox: A MATLAB Toolbox for

756 Relating Neural Signals to Continuous Stimuli. *Frontiers in Human*

757 *Neuroscience*, 10(November), 604. <https://doi.org/10.3389/fnhum.2016.00604>

758 Daube, C., Ince, R. A. A., & Gross, J. (2019). Simple Acoustic Features Can Explain
759 Phoneme-Based Predictions of Cortical Responses to Speech. *Current Biology*,
760 29(12), 1924-1937.e9. <https://doi.org/10.1016/j.cub.2019.04.067>

761 DeLong, K. A., Urbach, T. P., & Kutas, M. (2005). Probabilistic word pre-activation
762 during language comprehension inferred from electrical brain activity. *Nature
763 Neuroscience*, 8(8), 1117–1121. <https://doi.org/10.1038/nn1504>

764 DeWitt, I., & Rauschecker, J. P. (2012). Phoneme and word recognition in the
765 auditory ventral stream. *Proceedings of the National Academy of Sciences of the
766 United States of America*, 109(8), 505–514.
767 <https://doi.org/10.1073/pnas.1113427109>

768 Di Liberto, G. M., O’Sullivan, J. A., & Lalor, E. C. (2015). Low-frequency cortical
769 entrainment to speech reflects phoneme-level processing. *Current Biology*,
770 25(19), 2457–2465. <https://doi.org/10.1016/j.cub.2015.08.030>

771 Dikker, S., & Pylkkänen, L. (2013). Predicting language: MEG evidence for lexical
772 preactivation. *Brain and Language*, 127(1), 55–64.
773 <https://doi.org/10.1016/j.bandl.2012.08.004>

774 Ding, N., & Simon, J. Z. (2012). Emergence of neural encoding of auditory objects
775 while listening to competing speakers. *Proceedings of the National Academy of
776 Sciences of the United States of America*, 109(29), 11854–11859.
777 <https://doi.org/10.1073/pnas.1205381109>

778 Ding, N., & Simon, J. Z. (2014). Cortical entrainment to continuous speech:

779 functional roles and interpretations. *Frontiers in Human Neuroscience*, 8(May),

780 1–7. <https://doi.org/10.3389/fnhum.2014.00311>

781 Engel, A. K., & Fries, P. (2010). Beta-band oscillations--signalling the status quo?

782 *Current Opinion in Neurobiology*, 20(2), 156–165.

783 <https://doi.org/10.1016/j.conb.2010.02.015>

784 Engel, A. K., Fries, P., & Singer, W. (2001). Dynamic predictions: Oscillations and

785 synchrony in top–down processing. *Nature Reviews Neuroscience*, 2(10), 704–

786 716. <https://doi.org/10.1038/35094565>

787 Engel, A. K., Gerloff, C., Hilgetag, C. C., & Nolte, G. (2013). Intrinsic Coupling

788 Modes: Multiscale Interactions in Ongoing Brain Activity. *Neuron*, 80(4), 867–

789 886. <https://doi.org/10.1016/j.neuron.2013.09.038>

790 Federmeier, K. D. (2007). Thinking ahead: The role and roots of prediction in

791 language comprehension. *Psychophysiology*, 44(4), 491–505.

792 <https://doi.org/10.1111/j.1469-8986.2007.00531.x>.Thinking

793 Friederici, A. D. (2012). The cortical language circuit: From auditory perception to

794 sentence comprehension. *Trends in Cognitive Sciences*, 16(5), 262–268.

795 <https://doi.org/10.1016/j.tics.2012.04.001>

796 Fries, P. (2015). Rhythms for Cognition: Communication through Coherence.

797 *Neuron*, 88(1), 220–235. <https://doi.org/10.1016/j.neuron.2015.09.034>

798 Friston, K. (2005). A theory of cortical responses. *Philosophical Transactions of the*

799 *Royal Society B: Biological Sciences*, 360(1456), 815–836.

800 <https://doi.org/10.1098/rstb.2005.1622>

801 Friston, K. (2009). The free-energy principle: a rough guide to the brain? *Trends in*
802 *Cognitive Sciences*, 13(7), 293–301. <https://doi.org/10.1016/j.tics.2009.04.005>

803 Galindo-Leon, E. E., Stitt, I., Pieper, F., Stieglitz, T., Engler, G., & Engel, A. K.
804 (2019). Context-specific modulation of intrinsic coupling modes shapes
805 multisensory processing. *Science Advances*, 5(4), 1–13.

806 <https://doi.org/10.1126/sciadv.aar7633>

807 George, M. S., Kutas, M., Martinez, A., & Sereno, M. I. (1999). Semantic
808 engagement in reading. *Brain*, 122, 1317–1325.

809 Giraud, A. L., & Poeppel, D. (2012). Cortical oscillations and speech processing:
810 Emerging computational principles and operations. *Nature Neuroscience*, 15(4),
811 511–517. <https://doi.org/10.1038/nn.3063>

812 Harris, A. M., Dux, P. E., & Mattingley, J. B. (2018). Detecting Unattended Stimuli
813 Depends on the Phase of Prestimulus Neural Oscillations. *The Journal of*
814 *Neuroscience*, 38(12), 3092–3101. <https://doi.org/10.1523/jneurosci.3006-17.2018>

815 17.2018

816 Hickok, G. (2012a). Computational neuroanatomy of speech production. *Nature*
817 *Reviews Neuroscience*, 13(january), 135–145. <https://doi.org/10.1038/nrn3158>

818 Hickok, G. (2012b). The cortical organization of speech processing: Feedback control

819 and predictive coding the context of a dual-stream model. *Journal of*
820 *Communication Disorders*, 45(6), 393–402.
821 <https://doi.org/10.1016/j.jcomdis.2012.06.004>

822 Hickok, G., Houde, J., & Rong, F. (2011). Sensorimotor Integration in Speech
823 Processing: Computational Basis and Neural Organization. *Neuron*, 69(3), 407–
824 422. <https://doi.org/10.1016/j.neuron.2011.01.019>

825 Hisagi, M., Shafer, V. L., Strange, W., & Sussman, E. S. (2015). Neural measures of a
826 Japanese consonant length discrimination by Japanese and American English
827 listeners: Effects of attention. *Brain Research*, 1626, 218–231.
828 <https://doi.org/10.1016/j.brainres.2015.06.001>

829 Huang, Q., Jia, J., Han, Q., & Luo, H. (2018). Fast-backward replay of sequentially
830 memorized items in humans. *eLife*, 7(e35164), 376202.
831 <https://doi.org/10.7554/eLife.35164.001>

832 Iemi, L., Busch, N. A., Laudini, A., Haegens, S., Samaha, J., Villringer, A., &
833 Nikulin, V. V. (2019). Multiple mechanisms link prestimulus neural oscillations
834 to sensory responses. *eLife*, 8(e43620), 461558. <https://doi.org/10.1101/461558>

835 Jehee, J. F. M., & Ballard, D. H. (2009). Predictive feedback can account for biphasic
836 responses in the lateral geniculate nucleus. *PLoS Computational Biology*, 5(5).
837 <https://doi.org/10.1371/journal.pcbi.1000373>

838 Jensen, O., & Mazaheri, A. (2010). Shaping functional architecture by oscillatory
839 alpha activity: Gating by inhibition. *Frontiers in Human Neuroscience*,

840 4(November), 1–8. <https://doi.org/10.3389/fnhum.2010.00186>

841 Kayser, S. J., Ince, R. A. A., Gross, J., & Kayser, C. (2015). Irregular Speech Rate

842 Dissociates Auditory Cortical Entrainment, Evoked Responses, and Frontal

843 Alpha. *Journal of Neuroscience*, 35(44), 14691–14701.

844 <https://doi.org/10.1523/JNEUROSCI.2243-15.2015>

845 Keitel, A., Gross, J., & Kayser, C. (2018). Perceptually relevant speech tracking in

846 auditory and motor cortex reflects distinct linguistic features. *PLoS Biology*,

847 16(3), 1–19. <https://doi.org/10.1371/journal.pbio.2004473>

848 Klimesch, W. (2012). Alpha-band oscillations, attention, and controlled access to

849 stored information. *Trends in Cognitive Sciences*, 16(12), 606–617.

850 <https://doi.org/10.1016/j.tics.2012.10.007>

851 Klimesch, W., Sauseng, P., & Hanslmayr, S. (2007). EEG alpha oscillations: The

852 inhibition-timing hypothesis. *Brain Research Reviews*, 53(1), 63–88.

853 <https://doi.org/10.1016/j.brainresrev.2006.06.003>

854 Kok, P., Jehee, J. F. M., & de Lange, F. P. (2012). Less Is More: Expectation

855 Sharpens Representations in the Primary Visual Cortex. *Neuron*, 75(2), 265–270.

856 <https://doi.org/10.1016/j.neuron.2012.04.034>

857 Kok, P., Mostert, P., & De Lange, F. P. (2017). Prior expectations induce prestimulus

858 sensory templates. *Proceedings of the National Academy of Sciences of the*

859 *United States of America*, 114(39), 10473–10478.

860 <https://doi.org/10.1073/pnas.1705652114>

861 Kok, P., Rahnev, D., Jehee, J. F. M., Lau, H. C., & de Lange, F. P. (2012). Attention
862 Reverses the Effect of Prediction in Silencing Sensory Signals. *Cerebral Cortex*,
863 22(9), 2197–2206. <https://doi.org/10.1093/cercor/bhr310>

864 Kutas, M., & Federmeier, K. D. (2011). Thirty Years and Counting: Finding Meaning
865 in the N400 Component of the Event-Related Brain Potential (ERP). *Annual
866 Review of Psychology*, 62(1), 621–647.
867 <https://doi.org/10.1146/annurev.psych.093008.131123>

868 Kutas, M., & Hillyard, S. A. (1984). Brain potentials during reading reflect word
869 expectancy and semantic association. *Nature*, 307(5947), 161–163.

870 Lakatos, P., O'Connell, M. N., Barczak, A., Mills, A., Javitt, D. C., & Schroeder, C.
871 E. (2009). The Leading Sense: Supramodal Control of Neurophysiological
872 Context by Attention. *Neuron*, 64(3), 419–430.
873 <https://doi.org/10.1016/j.neuron.2009.10.014>

874 Lalor, E. C., Pearlmuter, B. A., Reilly, R. B., McDarby, G., & Foxe, J. J. (2006). The
875 VESPA: A method for the rapid estimation of a visual evoked potential.
876 *NeuroImage*, 32(4), 1549–1561.
877 <https://doi.org/10.1016/j.neuroimage.2006.05.054>

878 Lau, E. F., Phillips, C., & Poeppel, D. (2008). A cortical network for semantics:
879 (de)constructing the N400. *Nature Reviews Neuroscience*, 9(12), 920–933.
880 <https://doi.org/10.1038/Nrn2532>

881 Luck, S. J., Woodman, G. F., & Vogel, E. K. (2000). Event-related potential studies

882 of attention. *Trends in Cognitive Sciences*, 4(11), 432–440.

883 [https://doi.org/10.1016/S1364-6613\(00\)01545-X](https://doi.org/10.1016/S1364-6613(00)01545-X)

884 Luo, H., & Poeppel, D. (2007). Phase Patterns of Neuronal Responses Reliably
885 Discriminate Speech in Human Auditory Cortex. *Neuron*, 54(6), 1001–1010.

886 <https://doi.org/10.1016/j.neuron.2007.06.004>

887 Maris, E., & Oostenveld, R. (2007). Nonparametric statistical testing of EEG- and
888 MEG-data. *Journal of Neuroscience Methods*, 164(1), 177–190.

889 <https://doi.org/10.1016/j.jneumeth.2007.03.024>

890 Marzecová, A., Widmann, A., SanMiguel, I., Kotz, S. A., & Schröger, E. (2017).
891 Interrelation of attention and prediction in visual processing: Effects of task-
892 relevance and stimulus probability. *Biological Psychology*, 125, 76–90.

893 <https://doi.org/10.1016/j.biopsych.2017.02.009>

894 Mathewson, K. E., Lleras, A., Beck, D. M., Fabiani, M., Ro, T., & Gratton, G. (2011).
895 Pulsed out of awareness: EEG alpha oscillations represent a pulsed-inhibition of
896 ongoing cortical processing. *Frontiers in Psychology*, 2(MAY), 1–15.

897 <https://doi.org/10.3389/fpsyg.2011.00099>

898 Milton, A., & Pleydell-Pearce, C. W. (2016). The phase of pre-stimulus alpha
899 oscillations influences the visual perception of stimulus timing. *NeuroImage*,
900 133, 53–61. <https://doi.org/10.1016/j.neuroimage.2016.02.065>

901 Mirkovic, B., Bleichner, M. G., De Vos, M., & Debener, S. (2016). Target speaker
902 detection with concealed EEG around the ear. *Frontiers in Neuroscience*,

903 10(JUL), 1–11. <https://doi.org/10.3389/fnins.2016.00349>

904 Mirkovic, B., Debener, S., Jaeger, M., & Vos, M. De. (2015). Decoding the attended

905 speech stream with multi-channel EEG: implications for online, daily-life

906 applications. *Journal of Neural Engineering*, 12(4), 046007.

907 <https://doi.org/10.1088/1741-2560/12/4/046007>

908 Nobre, A. C., & Van Ede, F. (2018). Anticipated moments: Temporal structure in

909 attention. *Nature Reviews Neuroscience*, 19(1), 34–48.

910 <https://doi.org/10.1038/nrn.2017.141>

911 O’Sullivan, J. A., Power, A. J., Mesgarani, N., Rajaram, S., Foxe, J. J., Shinn-

912 Cunningham, B. G., ... Lalor, E. C. (2015). Attentional Selection in a Cocktail

913 Party Environment Can Be Decoded from Single-Trial EEG. *Cerebral Cortex*,

914 25(7), 1697–1706. <https://doi.org/10.1093/cercor/bht355>

915 Oostenveld, R., Fries, P., Maris, E., & Schoffelen, J. (2011). FieldTrip : Open Source

916 Software for Advanced Analysis of MEG , EEG , and Invasive

917 Electrophysiological Data. *Computational Intelligence and Neuroscience*, 2011.

918 <https://doi.org/10.1155/2011/156869>

919 Pisoni, D. B., & Luce, P. A. (1987). Acoustic-phonetic representations in word

920 recognition. *Cognition*, 25(1–2), 21–52. [https://doi.org/10.1016/0010-0277\(87\)90003-5](https://doi.org/10.1016/0010-0277(87)90003-5)

922 Rao, R. P. N., & Ballard, D. H. (1999). Predictive coding in the visual cortex: A

923 functional interpretation of some extra-classical receptive-field effects. *Nature*

924 *Neuroscience*, 2(1), 79–87. <https://doi.org/10.1038/4580>

925 Rassi, E., Wutz, A., Müller-Voggel, N., & Weisz, N. (2019). Prestimulus feedback

926 connectivity biases the content of visual experiences. *Proceedings of the*

927 *National Academy of Sciences*, 116(32), 16056–16061.

928 <https://doi.org/10.1073/pnas.1817317116>

929 Robertson, D. A., Gernsbacher, M. A., Guidotti, S. J., Robertson, R. R. W., Irwin, W.,

930 Mock, B. J., & Campana, M. E. (2000). Functional neuroanatomy of the

931 cognitive process of mapping during discourse comprehension. *Psychological*

932 *Science*, 11(3), 255–260. <https://doi.org/10.1111/1467-9280.00251>

933 Rohenkohl, G., & Nobre, A. C. (2011). Alpha Oscillations Related To Anticipatory

934 Attention Follow Temporal Expectations. *The Journal of Neuroscience : The*

935 *Official Journal of the Society for Neuroscience*, 31(40), 14076–14084.

936 <https://doi.org/10.1523/JNEUROSCI.3387-11.2011>

937 Rommers, J., Dickson, D. S., Norton, J. J. S., Wlotko, E. W., & Federmeier, K. D.

938 (2017). Alpha and theta band dynamics related to sentential constraint and word

939 expectancy. *Language, Cognition and Neuroscience*, 32(5), 576–589.

940 <https://doi.org/10.1080/23273798.2016.1183799>

941 Salinas, E., & Sejnowski, T. J. (2001). Correlated neuronal activity and the flow of

942 neural information. *Nature Reviews Neuroscience*, 2(8), 539–550.

943 <https://doi.org/10.1038/35086012>

944 Sauseng, P., Klimesch, W., Gruber, W. R., Hanslmayr, S., Freunberger, R., &

945 Doppelmayr, M. (2007). Are event-related potential components generated by
946 phase resetting of brain oscillations? A critical discussion. *Neuroscience*, 146(4),
947 1435–1444. <https://doi.org/10.1016/j.neuroscience.2007.03.014>

948 Schröger, E., Kotz, S. A., & SanMiguel, I. (2015). Bridging prediction and attention
949 in current research on perception and action. *Brain Research*, 1626, 1–13.
950 <https://doi.org/10.1016/j.brainres.2015.08.037>

951 Schröger, E., Marzecová, A., & Sanmiguel, I. (2015). Attention and prediction in
952 human audition: A lesson from cognitive psychophysiology. *European Journal
953 of Neuroscience*, 41(5), 641–664. <https://doi.org/10.1111/ejn.12816>

954 Schyns, P. G., Thut, G., & Gross, J. (2011). Cracking the code of oscillatory activity.
955 *PLoS Biology*, 9(5), 1001063. <https://doi.org/10.1371/journal.pbio.1001064>

956 Sedley, W., Gander, P. E., Kumar, S., Kovach, C. K., Oya, H., Kawasaki, H., ...
957 Griffiths, T. D. (2016). Neural signatures of perceptual inference. *eLife*,
958 5(MARCH2016), 1–13. <https://doi.org/10.7554/eLife.11476>

959 Smith, J. L., Johnstone, S. J., & Barry, R. J. (2006). Effects of pre-stimulus processing
960 on subsequent events in a warned Go/NoGo paradigm: Response preparation,
961 execution and inhibition. *International Journal of Psychophysiology*, 61(2), 121–
962 133. <https://doi.org/10.1016/j.ijpsycho.2005.07.013>

963 Smout, C. A., Tang, M. F., Garrido, M. I., & Mattingley, J. B. (2019). Attention
964 promotes the neural encoding of prediction errors. *PLoS Biology*, 17(2), 1–22.
965 <https://doi.org/10.1371/journal.pbio.2006812>

966 S öderström, P., Horne, M., Frid, J., & Roll, M. (2016). Pre-Activation Negativity
967 (PrAN) in Brain Potentials to Unfolding Words. *Frontiers in Human*
968 *Neuroscience*, 10(October), 1–11. <https://doi.org/10.3389/fnhum.2016.00512>

969 S öderström, P., Horne, M., Mannfolk, P., van Westen, D., & Roll, M. (2018). Rapid
970 syntactic pre-activation in Broca's area: Concurrent electrophysiological and
971 haemodynamic recordings. *Brain Research*, 1697, 76–82.
972 <https://doi.org/10.1016/j.brainres.2018.06.004>

973 Szewczyk, J. M., & Schriefers, H. (2018). The N400 as an index of lexical
974 preactivation and its implications for prediction in language comprehension.
975 *Language, Cognition and Neuroscience*, 33(6), 665–686.
976 <https://doi.org/10.1080/23273798.2017.1401101>

977 Tian, X., Ding, N., Teng, X., Bai, F., & Poeppel, D. (2018). Imagined speech
978 influences perceived loudness of sound. *Nature Human Behaviour*, 2(3), 225–
979 234. <https://doi.org/10.1038/s41562-018-0305-8>

980 van Ede, F., Jensen, O., & Maris, E. (2010). Tactile expectation modulates pre-
981 stimulus A-band oscillations in human sensorimotor cortex. *NeuroImage*, 51(2),
982 867–876. <https://doi.org/10.1016/j.neuroimage.2010.02.053>

983 Van Petten, C., & Luka, B. J. (2012). Prediction during language comprehension:
984 Benefits, costs, and ERP components. *International Journal of*
985 *Psychophysiology*, 83(2), 176–190.
986 <https://doi.org/10.1016/j.ijpsycho.2011.09.015>

987 Verhulst, S., Alto è, A., & Vasilkov, V. (2018). Computational modeling of the human
988 auditory periphery: Auditory-nerve responses, evoked potentials and hearing
989 loss. *Hearing Research*, 360, 55–75.

990 <https://doi.org/10.1016/j.heares.2017.12.018>

991 Zhang, D., Hong, B., Gao, S., & R öder, B. (2017). Exploring the temporal dynamics
992 of sustained and transient spatial attention using steady-state visual evoked
993 potentials. *Experimental Brain Research*, 235(5), 1575–1591.

994 <https://doi.org/10.1007/s00221-017-4907-6>

995 Zion Golumbic, E., Cogan, G. B., Schroeder, C. E., & Poeppel, D. (2013). Visual
996 input enhances selective speech envelope tracking in auditory cortex at a
997 “cocktail party”. *The Journal of Neuroscience*, 33(4), 1417–1426.

998 <https://doi.org/10.1523/JNEUROSCI.3675-12.2013>

999